JOURNAL OF SOLID STATE CHEMISTRY 64, 240–248 (1986)

Lithium Insertion Compounds of $LiFe_5O_8$, $Li_2FeMn_3O_8$, and $Li_2ZnMn_3O_8$

C. J. CHEN AND M. GREENBLATT*

Department of Chemistry, Rutgers, The State University of New Jersey, New Brunswick, New Jersey 08903

AND J. V. WASZCZAK

AT&T Bell Laboratories, Murray Hill, New Jersey 07974

Received October 4, 1985

Lithium insertion reactions of the lithium spinels $Fe[Li_{0.5}Fe_{1.5}]O_4$, $Li_{0.5}Zn_{0.5}[Li_{0.5}Mn_{1.5}]O_4$ and $Li[Fe_{0.5}Mn_{1.5}]O_4$ by *n*-butyl lithium or electrochemically yield $Li_{2.5}Fe_{2.5}O_4$, $Li_2Zn_{0.5}Mn_{1.5}O_4$, and $Li_2Fe_{0.5}Mn_{1.5}O_4$, respectively. It is shown that the $[B_2]O_4$ framework of the $A[B_2]O_4$ spinel structure remains intact upon lithium insertion, and provides a three-dimensional interstitial pathway for Li^+ ion diffusion. Lithium insertion is completely reversible in the normal lithium spinel $LiFe_{0.5}Mn_{1.5}O_4$; delithiation of $Li_{2.5}Fe_{2.5}O_4$ results in $Li_{1.5}Fe_{2.5}O_4$ and none of the inserted lithium may be removed from the mixed lithium spinel $Li_2Zn_{0.5}Mn_{1.5}O_4$. Physicochemical properties including electrical resistivity, magnetic susceptibility, and Mössbauer spectra of the hosts and their lithiated analogs are discussed.

Introduction

Topotactic lithium insertion/extraction, oxidation/reduction reactions have been demonstrated in a variety of spinel phases including Fe_3O_4 (*1*), Mn_3O_4 (*2*), Co_3O_4 (*3*), $LiMn_2O_4$ (*2, 4–7*), $LiTi_2O_4$ (*8–10*), and LiV_2O_4 (*8, 11*).

The ideal spinel structure, $A[B_2]O_4$ can be described as a cubic close-packed array of oxide ions in which only one-half of the octahedral and one-eighth of the tetrahedral sites are occupied. There are eight molecules per unit cell and oxygens are located at the 32*e* position of space group *Fd3m*. The *B* cations occupy octahedral sites at 16*d*, the empty octahedral sites are at 16*c*. The 64 tetrahedral interstices are at the three nonequivalent positions 8*a*, 8*b*, and 48*f*; the *A* cations occupy site 8*a*. Each 8*a* tetrahedron shares common faces with four neighboring empty 16*c* octahedra which allows a possible diffusion pathway for the *A* cations, 8*a* → 16*c* → 8*a* → 16*c* → etc., through the structure. In contrast, the 8*b* tetrahedra share faces with the 16*d* octahedra occupied by the *B* cations, which renders them energetically unfavorable for cation occupation. The 48*f* tetrahedra share faces with both 16*d* and empty 16*c* octahedra. A cation distribution of $A[B_2]O_4$ and $B[A,B]O_4$ is classified as a normal and inverse spinel, respectively. Mixed (or intermediate) spinels have a cation arrange-

* To whom correspondence should be addressed.

0022-4596/86 $3.00

ment corresponding to $A_xB_y(A_{1-x}B_{1-y})O_4$ (*12*).

It has been established by X-ray (*1*) and neutron diffraction (*10*) studies that the $[B_2]O_4$ sublattice of the $A[B_2]O_4$ spinel structure remains intact upon lithium insertion/extraction and provides a *three-dimensional* (3D) framework and an interstitial space of edge-shared octahedra connected in three dimensions for Li^+ ion diffusion as shown in Fig. 1. Previous studies indicate that on lithium insertion into spinel the lithium ions in $Li_xA[B_2]O_4$ occupy the octahedral 16*c* vacant sites up to $x = 1$ and the tetrahedral *A* (8*a*) cations are cooperatively displaced to octahedral 16*c* sites producing partially ordered rock salt-like phases, e.g., $\{LiFe\}[Fe_2]O_4$ where the curly bracket stands for the 16*c* octahedral sites. Additional lithium ions inserted ($1 \leq x \leq 2$) must therefore occupy the empty 8*a* and/or 48*f* sites (*1, 7, 10*). Because the Li^+ ions in these tetrahedral sites scatter X rays weakly, the fully lithiated phases $Li_2A[B_2]O_4$ also show a rock salt-like diffraction powder pattern. As mentioned earlier, the interconnected 16*c* and 8*a* (or 48*f*) sites form a continuous 3D pathway for Li^+ ion transport. Thus cations other than Li^+ in these sites will hinder more strongly the diffusion of inserted Li^+ ions due to coulombic considerations. We have studied the effect of cation distribution on the extent of lithium insertion in a series of iron spinels and found that the lithium content decreases in the order inverse > "mixed" > normal spinels (*13*). It appears that only in the inverse spinels, where a reducible cation ($Fe^{3+}[Fe^{2+}, Fe^{3+}]O_4$) is present in the 8*a* tetrahedral site, can more than one Li^+ ion be inserted per formula unit (e.g., $Li_2Fe_3O_4$ vs $LiMn_3O_4$). Furthermore, in these spinels Li^+ ions in excess of $x > 1$ can be removed by chemical or electrochemical delithiation ($LiFe_3O_4$ and $LiMn_3O_4$ cannot be delithiated) (*13*). In contrast, the normal lithium spinels with Li^+ ions in the 8*a* sites, $Li[B_2]O_4$ with B = Ti, V, Mn undergo lithium insertion reversibly to form $Li_2[B_2]O_4$ phases (*2–10*).

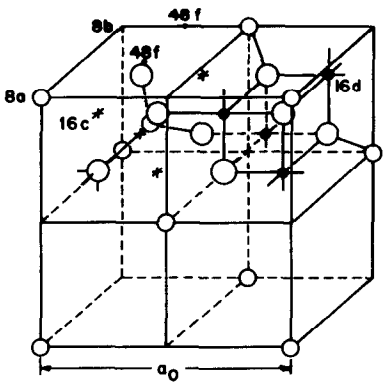

FIG. 1. Half a unit cell of the spinel structure (after Ref. (*7*)) showing the position of: (○) 8*a* and (●) 16*d* cations; (○) some of the 32*e* oxygens; 8*b*, (●) 48*f*, and (*) 16*c* interstitial sites in one quarter (two octants) of the unit cell.

In this paper we report lithium insertion reaction studies of three lithium spinels with different lithium content in the *A* site: $Fe[Li_{0.5}Fe_{1.5}]O_4$ (inverse, 0% Li^+ in 8*a*); $Zn_{0.5}Li_{0.5}[Li_{0.5}Mn_{1.5}O_4$ (mixed, 50% Li in 8*a*); $Li[Fe_{0.5}Mn_{1.5}]O_4$ (normal, 100% Li in 8*a*).

We have chosen these compounds to study the effect of Li^+ occupancy of the tetrahedral *A*(8*a*) sites on the lithium insertion reaction of spinel phases, particularly with respect to reversibility.

Experimental

$Fe[Li_{0.5}Fe_{1.5}]O_4$ (or $LiFe_5O_8$) was prepared according to Wickham (*14*). Fine powders of Fe_2O_3 and Li_2CO_3 (5 : 1 in mole ratio) mixed with Li_2SO_4 and Na_2SO_4 in a platinum crucible were calcined at 800°C for 1 hr in air, followed by washing away the salts with water. $Li_{0.5}Zn_{0.5}[Li_{0.5}Mn_{1.5}O_4$ (or $Li_2ZnMn_3O_8$) and $Li[Fe_{0.5}Mn_{1.5}]O_4$ (or $Li_2FeMn_3O_8$) were prepared after the method of Blasse by solid state reaction of stoichiometric mixtures of ZnO or Fe_2O_3,

Li_2CO_3, and $MnCO_3$, respectively (*15, 16*). Chemical treatment of the spinel phases with *n*-butyl lithium (*n*-BuLi) in dry hexane was carried out at room temperature with magnetic stirring for several days in a He-filled glovebox. The electrochemical lithiation was carried out in a small test cell (*17*) with Li metal as the anode, a mixture of one of the lithium host spinels and graphite (20 wt%) in the form of a compacted pellet as the cathode and 1 *M* $HClO_4$ in propylene carbonate (PC) as the electrolyte. Current densities of 10 to 30 $\mu A/cm^2$ were employed and the open circuit voltages (V) were recorded intermittently after equilibrium was reached as indicated by a constant potential. Delithiation of the lithiated compounds was performed with 2,3-dichloro-4,5-dicyanobenzoquinone in CH_3CN (DDQ/CH_3CN. The lithium content of the lithiated and delithiated compounds was determined by acid-base back-titration and/or plasma emission spectroscopy.

All the host spinels and reaction products were identified by powder X-ray diffraction methods using Ni-filtered copper radiation, with Si powder as internal standard. Samples were protected from air in a specially designed holder which was assembled in the drybox.

Magnetic susceptibilities were measured using the Faraday method as described previously (*18*). ^{57}Fe Mössbauer experiments were carried out in transmission geometry using a Pd(^{57}Co) source.

For two-probe measurement of qualitative electrical conductivities finely ground sample powders were pressed into thin pellets in a Teflon cylinder by two stainless-steel plungers which also served as the two leads.

Results and Discussion

$LiFe_5O_8$. On lithium insertion the red-brown color of α-$LiFe_5O_8$ changed to black in a few hours and a gradual loss of magnetic interaction of the powder with the magnetic stirrer was observed. The maximum lithium content of the fully lithiated product is $Li_{1+x}Fe_5O_8$, $x = 4$ (or $x = 2$ in $Li_{0.5+x}Fe_{2.5}O_4$). This is additional evidence that it is possible to insert two lithium ions into spinels when a reducible cation is present in the 8*a* tetrahedral site, as previously demonstrated in the inverse spinel ferrites, $Fe^{3+}[Fe^{2+}, Fe^{3}]O_4$ (*1*) and $Fe^{3+}[Ni^{2+}, Fe^{3+}]O_4$ (*13*). It appears that electron transfer from the inserted lithium atoms is facilitated when both the Li and the reducible metal ions (displaced from 8*a* to 16*c*) are in crystallographically equivalent positions (16*c*). Subsequent charge transfer ($x > 1$) which involves reduction of 16*d* transition metal ions may occur via $8a - 16d$, $d - p\ \pi$ interactions if the additional Li atoms go into the empty 8*a* sites, or via $48f - 16d$ interactions if the $x > 1$ Li atoms occupy 48*f* sites, or both of these may be operative; neutron diffraction powder profile analysis might resolve these ambiguities.

Powder X-ray diffraction data of the host lithium spinels and their lithiated analogs are summarized in Table I. The X-ray diffraction pattern of ordered α-$Fe_2^{3+}[Li Fe_3^{3+}]O_8$ was indexed based on space group $P4_33$ (No. 212) or $P4_13$ (No. 213) while that of $Li_5Fe_5O_8$ was indexed on the basis of space group $Fd3m$ (No. 227). The unit cell parameters were determined by least-squares refinement of the observed X-ray diffraction peaks. Insertion of lithium into $LiFe_5O_8$ results in a small expansion of the cubic cell dimension from 8.320 to 8.394 Å, which corresponds to ~2.6% increase in the unit cell volume. The X-ray intensity data (Table I) show that $Li_5Fe_5O_8$ has a structure similar to an FeO rock salt type (*19*). This indicates that in $Li_5Fe_5O_8$ as in lithiated Fe_3O_4 (*1*) and other lithiated spinel ferrites (*13*) a displacement of the *A*(8*a*) cations to the neighboring 16*c* octahedral site occurs. The inserted lithium ions are

TABLE I

X-RAY DIFFRACTION POWDER DATA OF SELECTED LITHIUM SPINEL PHASES

Compound	$LiFe_5O_8$ inverse	$Li_5Fe_5O_8$[a]	$Li_2ZnMn_3O_8$ mixed	$Li_4ZnMn_3O_8$	$Li_2FeMn_3O_8$ normal	$Li_4FeMn_3O_8$
Lattice parameters (Å)	a_0 = 8.320(2)	a_0 = 8.394(3)	a_0 = 8.220(3)	a_0 = 8.118(2) c_0 = 9.220(2)	a_0 = 8.256(2)	a_0 = 8.123(2) c_0 = 9.077(2)
Space group	$P4_332$ or $P4_132$	$Fd3m$	$Fd3m$	$F4_1/ddm$	$Fd3m$	$F4_1/ddm$
h k l	I/Io	I/Io	I/Io	I/Io	I/Io	I/Io
1 1 0	13	—	—	—	—	—
1 1 1	<1	—	47	100	100	100
2 1 0	20	—	—	—	—	—
2 1 1	13	—	—	—	—	—
2 2 0	45	—	33	—	—	—
3 1 0	5	—	—	—	—	—
(1 1 3)[b]	—	—	—	(24)	—	(30)
3 1 1	100	—	100	21	59	30
2 2 2	<2	50	24	59	16	28
(0 0 4)[b]	—	—	—	(24)	—	(31)
4 0 0	26	100	27	76	61	49
3 3 1	—	—	—	—	12	—
4 2 2	15	—	—	—	—	—
3 3 3 5 1 1	31	—	20	—	20	—
(4 0 4)[b]	—	—	—	(47)	—	(36)
4 4 0	38	56	30	—	31	—
5 3 1	—	—	—	—	14	—

[a] Space group $Fm3m$ (No. 225) with $a = 1/2a_0 = 4.197$ is more appropriate for FeO type structure, but a supercell with $a_0 = 2 \times 4.197$ was used to allow comparison with $Fd3m$ spinel space group.

[b] Tegragonal indexing only.

assumed to be distributed on the remaining 16*c*, the emptied 8*a* and/or 48*f* interstitial sites. In general the cubic spinel-to-rock salt transition is accompanied by a decrease of the ratio of the 220/440 and an increase in the ratio of 400/422 diffraction intensities (I_{220}/I_{440}, I_{400}/I_{422}) as a result of the diffusion of strong-scattering cations from tetrahedral (8*a*) to octahedral (16*c*) sites as discussed previously (*1*). For $Li_5Fe_5O_8$, I_{220} and I_{422} are zero, which strongly suggest that only the weakly scattering Li^+ ions occupy the tetrahedral sites.

Delithiation of $Li_5Fe_5O_8$ by the strong oxidizing agent DDQ/CH_3CN (I_2/CH_3CN was ineffective) produced $Li_3Fe_5O_8$ (black) a rock salt type and as in $Li_2Fe_3O_4$ no more than one Li^+ per spinel formula could be removed.

Results of the electrochemical lithiation of $LiFe_5O_8$ summarized graphically in Fig. 2 are in good agreement with results of chemical lithiation. The plot of open-circuit voltage vs x for the Li/$LiFe_5O_8$ cell is similar to that of the Li/Fe_3O_4 cell. Both plots show a single-phase region for $0 < x < 2$ and a critical Li^+ ion concentration $x_c \sim 0.1$ for the onset of the tetrahedral Fe^{3+} ion dif-

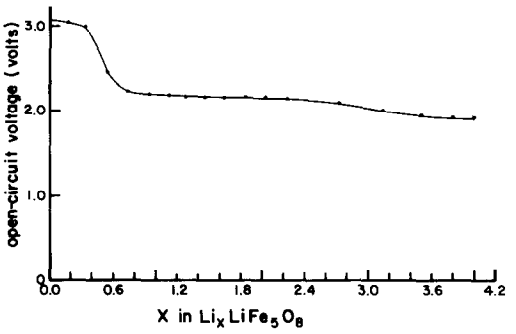

FIG. 2. Open-circuit voltage vs x for Li/1 M $LiClO_4$ PC/$Li_{1+x}Fe_5O_8$.

fusion to the 16*c* site. The plateau in the region of $0.4 \leq x \leq 0.9$ for $Li/Li_{0.5}Fe_{2.5}O_4$ may be due to the disordering of lithium and iron ions in the 16*d* site. The long equilibration time required to obtain stable open-circuit voltages in the cell after the current is discontinued is evidence that the diffusion rate of Li^+ ions in this spinel is slow as in other spinel ferrites.

Qualitative, two-probe electrical resistivity measurements at room temperature of $Li_5(Fe_4^{2+}Fe^{3+})O_8$ yield a value $\rho \sim 10$ Ω-cm, which is several orders of magnitude lower than that of the resistivity of the host, α-$LiFe_5^{3+}O_8$ ($\rho > 10^7$ Ω-cm) as expected for the mixed valent $Fe^{3+/2+}$ lithiated compound where electron hopping (or band conduction) might be responsible for the high conductivity observed.

The temperature variation of the magnetic susceptibility of $Li_5Fe_5O_8$ shown in Fig. 3 cannot be fit to a Curie–Weiss law in any range of the temperature measured (4.2–300 K). At low temperature ($T < 20$ K) the susceptibility saturates and exhibits a time dependence characteristic of a spin glass state (*20*). This behavior indicates that both ferromagnetic and antiferromagnetic interactions are present in a lattice of randomly distributed magnetic ions, and that the exchange energies are large.

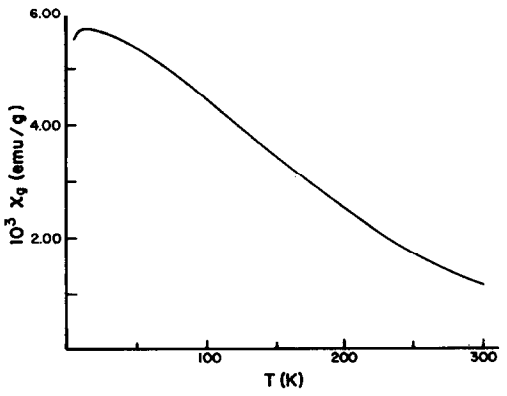

FIG. 3. Temperature variation of the magnetic susceptibility of $Li_5Fe_5O_8$.

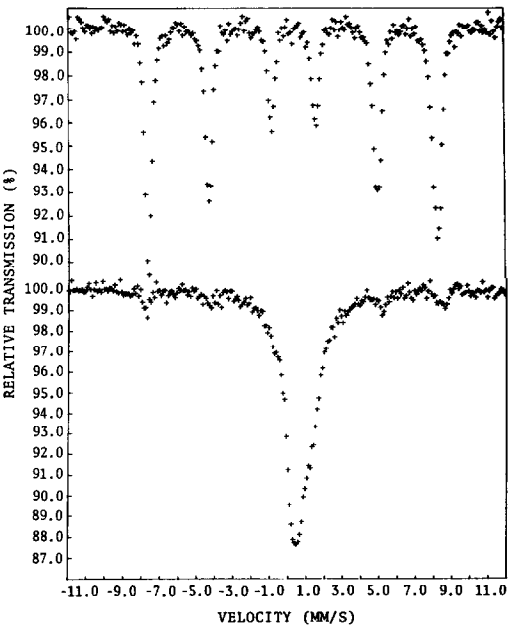

FIG. 4. ^{57}Fe Mössbauer spectra of $LiFe_5O_8$ and $Li_5Fe_5O_8$ (bottom) at 300 K.

The room-temperature ^{57}Fe Mössbauer spectrum of the magnetically ordered α-$Li_5Fe_5O_8$ is shown in Fig. 4. The observed spectrum of the host spinel is in good agreement with previously published results (*21*). The single broad resonance of the lithiated phase indicates that the magnetic ordering of the host is destroyed upon lithium insertion. The asymmetry and lineshape of the band suggest that iron in two different oxidation states (Fe^{2+}, Fe^{3+}) is present. However, the spectrum is not resolved sufficiently for a meaningful fit of the Mössbauer parameters. At low temperature ($T < 20$ K), the broad resonance of $Li_5Fe_5O_8$ splits into a complex multiline hyperfine pattern indicative of magnetic ordering. The shape and quality of the spectrum are typical of a disordered distribution of magnetic interactions in agreement with the magnetic susceptibility data.

$Li_2FeMn_3O_8$ and $Li_2ZnMn_3O_8$. Room-temperature lithium insertion of black $Li_2ZnMn_3O_8$ and $Li_2FeMn_3O_8$ by *n*-BuLi

yield $Li_4ZnMn_3O_8$ ($x = 1$ in $Li_{1+x}Zn_{0.5}Mn_{1.5}O_4$) and $Li_4FeMn_3O_8$ ($x = 1$ in $Li_{1+x}Fe_{0.5}Mn_{1.5}O_4$), respectively. No clear color change could be seen in the former sample, but a change to a red–brown color upon lithium insertion is observed in the latter.

Delithiation of the fully lithiated compound $Li_4FeMn_3O_8$ with excess DDQ/CH_3CN restores the original color and the cubic spinel phase of the host, $Li_2FeMn_3O_8$. Thus lithium insertion is reversible in ($Li[Fe_{0.5}Mn_{1.5}]O_4$) normal lithium spinel and is similar to the previously reported behavior of $Li[Mn_2]O_4$ (*2*), $Li[Ti_2]O_4$ (*8*), and $Li[V_2]O_4$ (*11*). In contrast, very little lithium can be removed from the fully lithiated "mixed" lithium spinel $Li_4ZnMn_3O_8$ (Table II); rather a mixture of phases, indicative of decomposition, were observed in samples delithiated by DDQ/CH_3CN.

The powder X-ray diffraction pattern of the host spinels, $Li_2ZnMn_3O_8$ and $Li_2FeMn_3O_8$, was indexed based on *Fd3m* (Table I) while those of their lithiated analogs fit the tetragonal space group $F4_1/ddm$ (alternate setting for $I4_1/amd$ space group No. 141). The absence of 220 reflection in all these phases except in $Li_2ZnMn_3O_8$ suggests that there are no strong X-ray scattering cations (Fe^{3+} or Zn^{2+}) in the 8*a* tetrahedral sites (i.e., probably $\{Li_2\}_{16c}[Fe_{0.5}Mn_{1.5}]_{16d}O_4$ and $\{Li_{1.5}Zn_{0.5}\}_{16c}[Li_{0.5}Mn_{1.5}]_{16d}O_4$ result upon lithiation).

The X-ray diffraction data for $Li_4ZnMn_3O_8$ and $Li_4FeMn_3O_8$ (Table I) show the tetragonal distortion present due to the cooperative Jahn-Teller effect of octahedrally coordinated $Mn^{3+}(d^4)$ compounds (*22*). The axial ratios (c/a) are 1.135 and 1.117 for $Li_4ZnMn_3O_8$ and $Li_4FeMn_3O_8$, respectively. This is direct evidence that the charge compensating electrons that accompany Li^+ insertion are transferred to the Mn^{4+} ions and thereby increase the concentration of the $Mn^{3+}(d^4)$ ions beyond the critical concentration (usually ~one Mn^{3+} ion per spinel formula) necessary for the onset of the Jahn-Teller distortion. It has been shown that there is no clear-cut relationship between the concentration of the Mn^{3+} ions

TABLE II

SUMMARY OF RESULTS OF LITHIUM/EXTRACTION IN SELECTED LITHIUM SPINEL PHASES

Compound	a_0[a] (Å)	x[b]	a, c, and c/a[c] (Å)	x_1[d]	a_2[e] (Å)	Reversibility	Ref.
α-$Fe^{3+}[Li_{0.5}Fe^{3+}_{1.5}]O_4$ (α-$LiFe_5O_8$)	8.320(2)	1.8 ± 0.2	a = 8.394(2)	1.5 ± 0.1	8.370(3)	Partial	This work
$Li_{0.5}Zn_{0.5}[Li_{0.5}Mn^{4+}_{1.5}]O_4$	8.220(2)	1.0 ± 0.2	a = 8.118(2)		—	Partial	This work
			c = 9.220(4)	~2.0 ± 0.1			
($Li_2ZnMn_3O_8$)			c/a = 1.135				
$Li_{1.0}[Fe^{3+}_{0.5}Mn^{3+}_{0.5}Mn^{4+}_{1.0}]O_4$	8.256(2)	1.0 ± 0.2	a = 8.123(2)	1.0	8.257(2)	Complete	This work
			c = 9.077(4)				
($Li_2FeMn_3O_8$)			c/a = 1.117				
$Li_{1.0}[Ti^{3+}Ti^{4+}]O_4$	8.410	1.0 ± 0.2	8.348	1.0[f]	8.410	Complete	*8*
$Li_{1.0}[Mn^{3+}Mn^{4+}]O_4$	8.242	1.0 ± 0.2	a = 8.007	1.0[g]	8.207	Complete	This work
			c = 9.274				
			c/a = 1.161				

[a] Lattice cell parameter of the host.
[b] Lithium ions inserted per formula spinel.
[c] Lattice parameters for the lithiated compounds.
[d] Residual lithium ions after delithiation of the fully lithiated compounds.
[e] Lattice parameters for the delithiated compounds.
[f] $LiTi_2O_4$ delithiated with I_2/CH_3CN yields $Li_{0.1}TiO_2$ which is a disordered, defect rock salt structure (*9*).
[g] Acid treatment of $Li[Mn_2]O_4$ yields $Li_{0.02}[Mn_2]O_4$ (*6*).

and the magnitude of the Jahn-Teller distortion (*23*). In the present compounds the importance of other cations in the 16*d* site effecting Jahn-Teller distortion is demonstrated again: $Li_3Zn[LiMn_2^{3+}Mn^{4+}]O_8$ is more distorted than $Li_4[Fe^{3+}Mn_3^{3+}]O_8$.

The room-temperature ^{57}Fe Mössbauer spectrum of $Li_2FeMn_3O_8$ and its lithiated analog in Fig. 5 show conclusively that the oxidation state of iron is 3+ in both the host and lithiated phases. The symmetrical doublet in each spectrum (Fig. 5) is characteristic of high-spin Fe^{3+} ions (isomer shift $\simeq$0.3 mm/sec and quadrupole splitting $\simeq$1.0 mm/sec). These results demonstrate that the Mn^{4+} ions are more readily reduced than Fe^{3+} or Mn^{3+} upon lithium insertion/reduction in spinels.

The magnetic susceptibility of $Li_2FeMn_3O_8$ and $Li_4FeMn_3O_8$ measured 4.2–300 K shown in Fig. 6 cannot be fit to a Curie–Weiss law with meaningful magnetic parameters in any range of the measured temperatures. At very low temperature ($T < 20$ K) the saturation and time dependence of the susceptibility of the host $Li_2FeMn_3O_8$ compound is characteristic of a spin glass state (*20*). There is no evidence of this state in the lithiated phase down to 4.2 K even though the data indicate a disordered distribution of strong magnetic interactions.

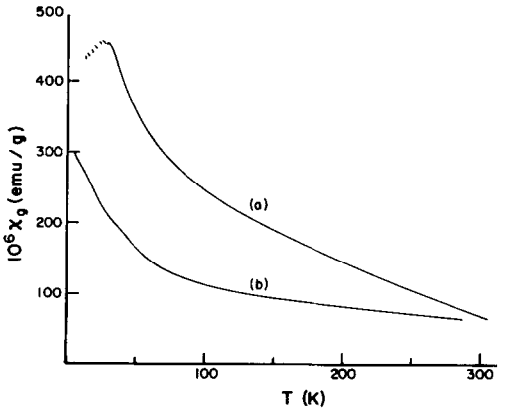

FIG. 6. Temperature variation of the magnetic susceptibility of (a) $Li_2FeMn_3O_8$ and (b) $Li_4FeMn_3O_8$.

The plot of open-circuit voltage (V) vs lithium composition (x) for the Li/Li$[Fe_{0.5}Mn_{1.5}]O_4$ cell is shown in Fig. 7. The shape of this plot is very similar to that observed for the Li/Li$[Mn_2]O_4$ cell (*2*). This is not unexpected since both host spinels are 100% normal (i.e., only Li^+ ions in tetrahedral 8*a* sites) and both of their lithiated compounds exhibit a Jahn-Teller tetragonal distortion ($c/a > 1$). The plateau in the V vs x plot represents a cubic/tetragonal two-

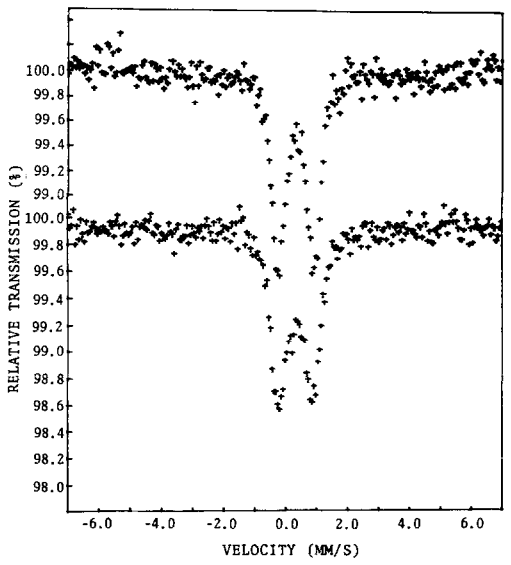

FIG. 5. ^{57}Fe Mössbauer spectra of $Li_2FeMn_3O_8$ and $Li_4FeMn_3O_8$ at 300 K.

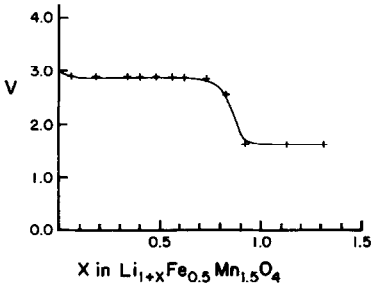

FIG. 7. Open-circuit voltage vs x for Li/1 *M* $LiClO_4$ PC/$Li_{2+x}FeMn_3O_8$.

phase region in the compositional range $0.06 < x < 0.7$. Since the cubic-to-tetragonal phase transformation is first-order, this two-phase region separates the cubic ($0 \leq x_c \leq 0.06$) and the tetragonal ($x \geq 0.7$) single phases. As indicated by Goodenough *et al.* (*7*), this type of two-phase region in electrochemical cells can provide high energy density instead of reducing the power performance of the electrode materials. This is because the Jahn-Teller distortion occurring in the course of lithium insertion represents a diffusionless phase transition with a strain-free phase boundary; hence, the motion of phase boundary may be faster than the diffusion of the Li^+ ions in the 3D interconnected interstitial space.

Room-temperature qualitative two-probe electrical resistivity measurements of $Li_2FeMn_3O_8$ and $Li_4FeMn_3O_8$ show that the resistivity of the host ($\rho \sim 10^3$ Ω-cm) dramatically increases upon lithiation ($\rho > 10^7$ Ω-cm for $Li_4FeMn_3O_8$). Similar measurements of the resistivity of $Li_2ZnMn_3O_8$ and $Li_4ZnMn_3O_8$ showed a marked decrease in the resistivity of the lithiated phase. These results support the assignment of the oxidation states of the ions as $Li_4Fe^{3+}Mn_3^{3+}O_8$ and $Li_4Zn(Mn_2^{3+}Mn^{4+})O_8$ as discussed before, and indicate that mobile *d* electrons in the mixed valent $Li_2Fe^{3+}(Mn_2^{4+}Mn^{3+})O_8$ host and $Li_4Zn(Mn_2^{3+}Mn^{4+})O_8$ lithiated compounds are responsible for the low resistivities.

Conclusions

From the results of lithium insertion/extraction in the three title lithium spinels summarized in Table II (along with data for $Li[Ti_2]O_4$ and $Li[Mn_2]O_4$) the following conclusions may be made:

1. The higher lithium uptake upon lithium insertion reactions of the inverse spinel $Fe^{3+}[Li_{0.5}Fe_{1.5}^{3+}]O_4$ (α-$LiFe_5O_8$) relative to the other two lithium spinels studied here is further evidence that lithium insertion into spinels is facilitated by the presence of readily reducible cations in the 8*a* tetrahedral sites as previously demonstrated in other inverse spinel ferrites, Fe_3O_4 (*1*) and $Fe[NiFe]O_4$ (*13*). This is probably due to the ease of electron transfer from the inserted Li atoms to the reducible transition metal ions when both are in crystallographically equivalent positions at 16*c*. If the additional ($x > 1$) Li atoms enter the 48*f* sites which share faces with the 16*d* octahedra, an easy path of charge transfer for the reduction of transition metal ions at that site may be accounted for.

2. There is direct evidence of electron transfer from the inserted lithium to reducible transition metal cations in the spinel by the onset of the cooperative Jahn-Teller effect in the manganese spinels due to increase of the Mn^{3+}/Mn^{4+} ratio as previously observed in related spinels (*2*).

3. Mössbauer data confirm that in $Li[Fe_{0.5}^{3+}Mn_{0.5}^{3+}Mn^{4+}]O_4$, ($Li_2FeMn_3O_8$) Mn^{4+}, rather than Fe^{3+} or Mn^{3+} ions are reduced upon lithium insertion.

4. $Li_2FeMn_3O_8$ may be a good cathode material for secondary lithium batteries since (a) the lithium insertion process is reversible and (b) the $Li/Li_2FeMn_3O_8$ cell exhibits a composition-independent open-circuit voltage of ~3.0 V against metallic lithium over the range $0.06 \leq x \leq 0.7$.

5. Only 100% normal lithium spinels such as $Li_2FeMn_3O_8$, $LiTi_2O_4$, LiV_2O_4, and $LiMn_2O_4$ display complete reversibility in room-temperature lithium insertion reactions.

Acknowledgments

We are grateful to R. H. Herber and H. Eckert for obtaining the Mössbauer data and their help with the interpretation of the Mössbauer results. Also we thank F. J. DiSalvo and D. W. Murphy for helpful discussions. This work was supported by the Office of Naval Research.

References

1. M. M. THACKERAY, W. I. F. DAVID, AND J. B. GOODENOUGH, *Mater. Res. Bull.* **17,** 785 (1982).
2. M. M. THACKERAY, W. I. F. DAVID, P. G. BRUCE, AND J. B. GOODENOUGH, *Mater. Res. Bull.* **18,** 461 (1983).
3. M. M. THACKERAY, S. D. BAKER, K. T. ADENDORFF, AND J. B. GOODENOUGH, *Solid State Ionics* **17,** 175 (1985).
4. J. C. HUNTER, *J. Solid State Chem.* **39,** 142 (1981).
5. A. MOSBAH, A. VERBAERE, AND M. TOURNOUX, *Mater. Res. Bull.* **18,** 1375 (1983).
6. M. M. THACKERAY, P. J. JOHNSON, L. A. DE PICCIOTTO, P. G. BRUCE, AND J. B. GOODENOUGH, *Mater. Res. Bull.* **19,** 179 (1984).
7. J. B. GOODENOUGH, M. M. THACKERAY, W. I. F. DAVID, AND P. G. BRUCE, *Rev. Chim. Miner.* **21,** 435 (1984).
8. D. W. MURPHY, M. GREENBLATT, S. M. ZAHURAK, R. J. CAVA, J. V. WASZCZAK, G. W. HULL, AND R. S. HUTTON, *Rev. Chim. Miner.* **19,** 441 (1982).
9. D. W. MURPHY, R. J. CAVA, S. M. ZAHURAK, AND A. SANTORO, *Solid State Ionics* **9,** and **10,** 413 (1983).
10. R. J. CAVA, D. W. MURPHY, AND S. ZAHURAK, *J. Solid State Chem.* **53,** 64 (1984).
11. L. A. DE PICCIOTTO AND M. M. THACKERAY, *Mater. Res. Bull.* **20,** 187 (1985).
12. A. F. WELLS, "Structural Inorganic Chemistry," p. 593, Clarendon Press, Oxford (1984).
13. C. J. CHEN, M. GREENBLATT AND J. V. WASZCZAK, *Solid State Ionics* **18, 19,** 838 (1986).
14. D. G. WICKHAM, *in* "Proc. Int. Conference on Ferrites, 1970," p. 105, Univ. Park Press, Tokyo (1971).
15. G. BLASSE, *J. Inorg. Nucl. Chem.* **25,** 703 (1963).
16. G. BLASSE, *Philips Res. Rep.* **20,** 528 (1965).
17. D. W. MURPHY, J. N. CARIDES, F. J. DISALVO, C. CROS, AND J. V. WASZCZAK, *Mater. Res. Bull.* **12,** 825 (1977).
18. F. J. DISALVO AND J. V. WASZCZAK, *Phys. Rev. B* **23,** 457 (1981).
19. ASTM Power diffraction file 6-615.
20. P. J. FORD, *Contemp. Phys.* **23,** 141 (1982).
21. B. LEREBOURS AND M. LENGLET, *Ann. Chim. Fr.* **4,** 347 (1979); N. K. Gill and R. K. Puri, *Spectrochim. Acta Part A* **41,** 1005 (1985).
22. J. B. GOODENOUGH AND A. L. LOEB, *Phys. Rev.* **98,** 391 (1955).
23. D. G. WICKHAM AND W. J. CROFT, *J. Phys. Chem. Solid* **7,** 351 (1958).